EXPERIMENTAL DEMONSTRATION OF A NOVEL SUPERCRITICAL CO_2 SEAL CONCEPT ON A 2″ STATIC TEST RIG

Mohammad Fuad Hassan
Georgia Southern University
Statesboro, USA

Hanping Xu
Ultool, LLC
Duluth, USA

Mohammad Towhidul Islam
Georgia Southern University
Statesboro, USA

Sevki Cesmeci*
Georgia Southern University
Statesboro, USA

Shuangbiao Liu
Ultool, LLC
Duluth, USA

Aaron Harcrow
Ultool, LLC
Duluth, USA

Ali Akbor Topu
Georgia Southern University
Statesboro, USA

Md Wasif Hasan
Georgia Southern University
Statesboro, USA

Jonah Henry
Georgia Southern University
Statesboro, USA

Joshua Bunting
Georgia Southern University
Statesboro, USA

David Dewis
Independent Consultant
New Hampshire, USA

Jing Tang
Ultool, LLC
Duluth, USA

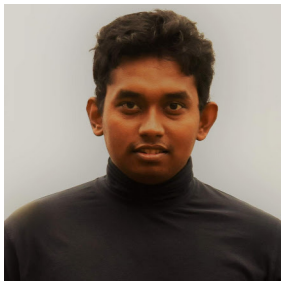

Mohammad Fuad Hassan

Mohammad Fuad Hassan currently works as a full time Research Engineer in the Mechanical Engineering Department at Georgia Southern University. He has been involved in projects funded by the Department of Energy and Juvenile Diabetes Research Foundation. Specifically, he has worked on novel sealing technologies for supercritical carbon dioxide power cycles and an innovative micropump design for insulin delivery applications. Fuad holds a B.S. degree from KUET and an M.S. degree from Georgia Southern University.

Hanping Xu

Dr. Hanping Xu is the President and the CEO of the Ultool, LLC. Dr. Xu has two decades of experience in tribology, seals, and plasma technology. He is innovative in developing pumps, seals, and other fluidic components for extreme conditions: ultrahigh high pressure, high speed, high temperature, and deep vacuum.

Mohammad Towhidul Islam

Mohammad Towhidul Islam is a Graduate Research Assistant in the Mechanical Engineering Department at Georgia Southern University since Spring 2022. He has been working on a novel elastohydrodynamic sealing technology for supercritical CO_2 power cycles and microfluidic devices for drug delivery applications. Prior to Georgia Southern, he had accumulated over five years of research experience in alternative fuels, emission control, and combustion.

Sevki Cesmeci

Dr. Sevki Cesmeci is an Assistant Professor of Mechanical Engineering at Georgia Southern University since Fall 2019. His research focuses on innovative sealing technologies for supercritical carbon dioxide power generation and aircraft engines, smart materials and structures, and novel high performance liquid chromatography pump designs. He has been the Principal Investigator of several government and nongovernment funded projects from the Department of Defense, Department of Energy, and Juvenile Diabetes Research Foundation.

Shuangbiao Liu

Dr. Shuangbiao (Jordan) Liu is an STLE fellow and a Research Professor at Northwestern University. He has worked at Caterpillar Inc. for 15 years to develop advanced tribological interfaces and hydraulic pumps/systems. His research interests mainly focus on tribological modelling, particularly on contact mechanics and mixed elastohydrodynamic lubrication involving rough surfaces, inclusions, coatings, and thermal aspects. His fast Fourier Transform based method – DC-FFT, along with a suite of fundamental solutions, has been widely applied in the tribological field to determine deformation/lubrication/stress/temperature field.

Aaron Harcrow

Aaron Harcrow is a multidisciplinary engineer having extensive skills in aircraft design, systems engineering, project management, research and development, electromechanical system design, rapid prototyping and manufacturing and CAD/CAM/CNC. These skills have been employed across multiple industries, including Lockheed Martin, Delta Air Lines, NASA Langley Research Center, academic institutions such as Mississippi State University, Georgia Tech and Southern Polytechnic State University and small businesses such as Ultool LLC, Commuter Craft LLC, Accurate Automation and Millennium Dynamics. Aaron received his M.S. and B.S. degrees in Aerospace Engineering from Georgia Tech and Mississippi State University, respectively.

Ali Akbor Topu

Ali Akbor Topu, is a Graduate Assistant at Georgia Southern University and is persuing his masters in mechanical engineering. His research is centered around novel sealing technologies for supercitical CO_2 power generation. This includes the numerical and experimental study of a new elastohydrodynamic seal for high pressure, high temperature working conditions.

Md Wasif Hasan

Md Wasif Hasan is a Graduate Research Assistant at Georgia Southern University pursuing a master's degree in mechanical engineering. His current research focuses on the design of multistage innovative elastohydrodynamic seals for supercritical carbon dioxide turbomachinery and jet engines and innovative pumps for drug delivery purposes. Prior to that, he had three years of experience in mechanical components design, development, and tribology for reciprocating compressors.

Jonah Henry

Jonah Henry is a senior and an Undergraduate Research Assistant in the Mechanical Engineering Department at Georgia Southern University. He has been involved in the fabrication of an elastohydrodynamic seal for supercritical CO_2 applications for the last three years.

Joshua Bunting

Joshua Bunting is a graduate of Mechanical Engineering Program at Georgia Southern University. Currently he works as a Piping Engineer at Valdes Architecture & Engineering. During his time at Georgia Southern University, he worked on the fabrication of an elastohydrodynamic seal for supercritical CO_2 applications as an Undergraduate Research Assistant.

David Dewis

David Dewis is a consultant to startups with over 30 years of experience in advanced energy systems. He is proficient in Business Planning, Concept Design, Design, CDR, PDR, Risk Mitigation, Strategic Partnerships, Program Management, Cost Optimization, and Manufacturing. David holds a Mechanical Engineering Degree from Coventry University.

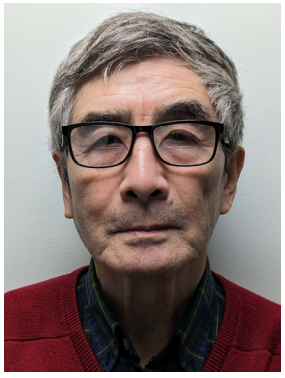

Jing Tang

Dr. Jing S Tang is a Principal Engineer at Ultool, LLC. He completed his PhD in the Department of Mechanical Engineering at the University of Leeds. Dr. Tang has extensive experience in scientific research and technology development at universities, institutions and international companies in the United States, the United Kingdom, and Germany.

ABSTRACT

Supercritical carbon dioxide (sCO_2) power cycles outperform conventional water-based/ air-breathing, direct-fired, open Brayton cycles or indirect-fired, closed Rankine cycles as far as the efficiency and equipment footprint are concerned. sCO_2 power cycles have promising potential to be used in concentrated solar power, fossil fuel power plants, geothermal electricity, nuclear power, and ship propulsion. Technology readiness must be proven on a scale of 10 – 600 MWe and at temperatures and pressures of 350–700°C and 20 – 35 MPa for nuclear industries, respectively, to realize the full potential of sCO_2 power cycles. One of the critical issues at the component level is the lack of effective shaft seals at sCO_2 operation conditions. While conventional seals are currently limited in some way by their inability to handle such high pressure and temperature, only a few non-conventional ones can survive sCO_2 conditions. To offer a potential solution, we propose an elastohydrodynamic (EHD) scalable high-temperature, high-pressure shaft end seal that leverages the proven elastohydrodynamic lubrication theory. The distinctive mechanism of such an EHD seal provides a self-regulated constriction effect to restrict the flow without significant material contact, thereby minimizing leakage and wear. One of the prominent features of the EHD seal is that it provides tighter sealing at increased pressures, sustaining a continuous fluid film between itself and the rotor. In this study, the working mechanism of the EHD seal was proven experimentally on a 2-in static rotor test rig. Tests were carried out using nitrogen as the working fluid at the room temperature to avoid complexity. The test seal was made of PEEK which had an elastic modulus of 3.65 GPa and a tensile strength of 96.53 MPa. The static shaft was made of stainless steel with a diameter of 2 in. The trials were run with a maximum inlet pressure of 15 MPa and an initial clearance of 41 μm. The throttling effect of the EHD seal was clearly demonstrated in these early trials. These preliminary findings suggest that the proposed EHD seal design can potentially be applied to sCO_2 turbomachinery.

Keywords: Seal; EHD seal; leakage; sCO_2; supercritical carbon dioxide; power generation

INTRODUCTION

Power generation has been and remains a focal point of economic, environmental, sociological, and ethical discourse in the field of engineering. In recent times, there has been a notable increase in the adoption of the sCO_2-based power cycle due to its favorable environmental attributes and cost-effectiveness [1]. In light of the continuously expanding global population and its corresponding electricity requirements, the closed-loop CO_2 power cycle is emerging as a promising and dependable alternative compared to other clean energy options [2]. Utilizing supercritical CO_2 as a working fluid offers significant advantages compared to conventional power generation approaches [3]–[8]. Its ability to maintain liquid density in the gaseous state, allows for a more cost-effective power cycle, better power density, and higher performance [9].

The existing seal and shaft solutions provide a higher level of compatibility with typical applications [10]–[11]. However, when it comes to sCO_2 operating conditions, the current sealing technology fails one way or another [12]–[14]. Despite considerable efforts to use the existing seals in sCO_2 power generation techniques, they require modifications from their conventional design [15]–[16]. In this list, dry gas and labyrinth seals have been the most popular ones [17]. Other important sealing technologies include brush seal, halo seal, shaft end seal etc. [18]–[23]. Among these, the labyrinth seal is considered more competitive because of its simple design than the dry gas seal [24]–[25]. The efficiency of each seal varies based on operational conditions and application, embracing both advantages and disadvantages. Yet, the non-contact seal has more significant requirements than the contact seal [26].

*Corresponding author
Sevki Cesmeci, PhD
scesmeci@georgiasouthern.edu

Several other sophisticated seal configurations have been developed and implemented, such as the film-riding seal, annular seal, hole-pattern seals, leaf seals, drum seals, hydrodynamic seals, and so on, specifically in the context of sCO_2 applications [27]–[34]. To date, traditional seals have encountered limitations in effectively managing the pressure and temperature of supercritical carbon dioxide (sCO_2) in various manners [26], [35]–[39]. That is why a worldwide effort exists to advance the development of efficient sealing methods for sCO_2 turbomachinery [40]–[46].

Wang et al. [47] investigated the relation between the leakage rate and the heat transfer properties of a labyrinth seal for varying shaft speeds and seal geometries. They ran a numerical analysis to identify the effect of rotation and varying geometrical parameters on the seal's performance. Although promising, they must still address their study's scalability and high operating condition issues. Untaroiu et al. [48] also conducted a computational analysis of a labyrinth seal's varying swirl break geometry properties. Based on their parametric sensitivity study, it has little effect on the overall efficiency of the seal.

Yuan et al. [49] studied the impact of dynamic groove types on the thermal characteristics and cooling effects on the sCO_2 dry gas seals in the industrial setting. They illustrated an external direct flush cooling method and showed a temperature reduction of 42.3%. By implementing sCO_2 real gas properties and solving 3D RANS equations, they successfully demonstrated the effect of the thermal characteristics of dynamic dry gas seals under varying coolant mass flow ratios.

Wang et al. [50] numerically investigated the steady performance of compliant foil seals at different operating parameters and pressure distribution. They analyzed a T-shaped seal groove and implemented the finite difference method to obtain the performance. Their study showed that the inlet pressure significantly influences the overall seal efficiency. It also addresses that to achieve damping and stiffness stability, the T-shaped groove needs to be optimized.

Elastohydrodynamic (EHD) characteristic analysis has been carried out in different studies as it plays a key role in the overall performance of the sealing technology. Nikas et al. [51]–[53] conducted a computational study on an elastomeric rectangular seal, focusing on EHD lubrication mechanics. The individual showcased a method for addressing these concerns without relying on pre-established compliance matrices or predetermined contact pressure. A separate investigation showcased the application of the Mooney-Rivlin rubber elasticity model to resolve EHD concerns. In this case, he formulated certain assumptions and implemented suitable modifications while considering the effects of temperature stressors. He then computed the numerical outcomes under various standard operating settings. Later, Stupkiewicz et al. [54] also studied a finite element analysis of various seals' deformation by coupling the fluid-solid interaction in EHD lubrication physics.

The elastic deformation of a sleeve seal enhances the sealing process's effectiveness and efficiency. Sleeve seals are the designated classification for high-pressure conformal EHD seals. Wong et al. [55] conducted a comprehensive investigation on the performance of high-pressure sleeve seals for reciprocating pumps using elastohydrodynamic (EHD) analysis. Estimating the leakage rate was also conducted to assess the influence of structural and operational factors. Their findings also provided insights into the impact of frictional force and stiffness on the performance of high-pressure sleeve seals. Additionally, the researchers proposed the implementation of the all-metal viscoelastic seal, an innovative sealing mechanism designed to withstand high-pressure conditions. They conducted an EHD lubrication analysis to evaluate the proposed high-pressure seal. The computation considered the deformation of the cylinder and

plunger and the relationship between the pressure-viscosity and density of the working fluid. Based on their research, the proposed seal is recommended to function consistently.

As a potentially viable sealing solution for sCO_2 turbomachinery, we present a patented elastohydrodynamic (EHD) shaft seal that operates under high-pressure and high-temperature conditions and possesses scalability, designed explicitly for sCO_2 cycles. According to the EHD mechanism, increased pressure results in a more effective sealing technique, maintaining a continuous sCO_2 film to prevent direct contact between the seal and the rotor. The EHD seal has a straightforward, sleeve-like configuration positioned concentrically to the rotor, including narrow clearances that are typically below 50 μm in magnitude. Due to its distinctive structural configuration, the pressure difference acting on the seal induces a constriction, forming a throat closer to the base of the seal. Our hypothesis posits that the throat functions as an efficient flow restrictor by achieving the minimal physically attainable clearance. The proposed EHD seal exhibits several advantages over current sealing technologies. These advantages include reduced leakage, decreased drag, minimized

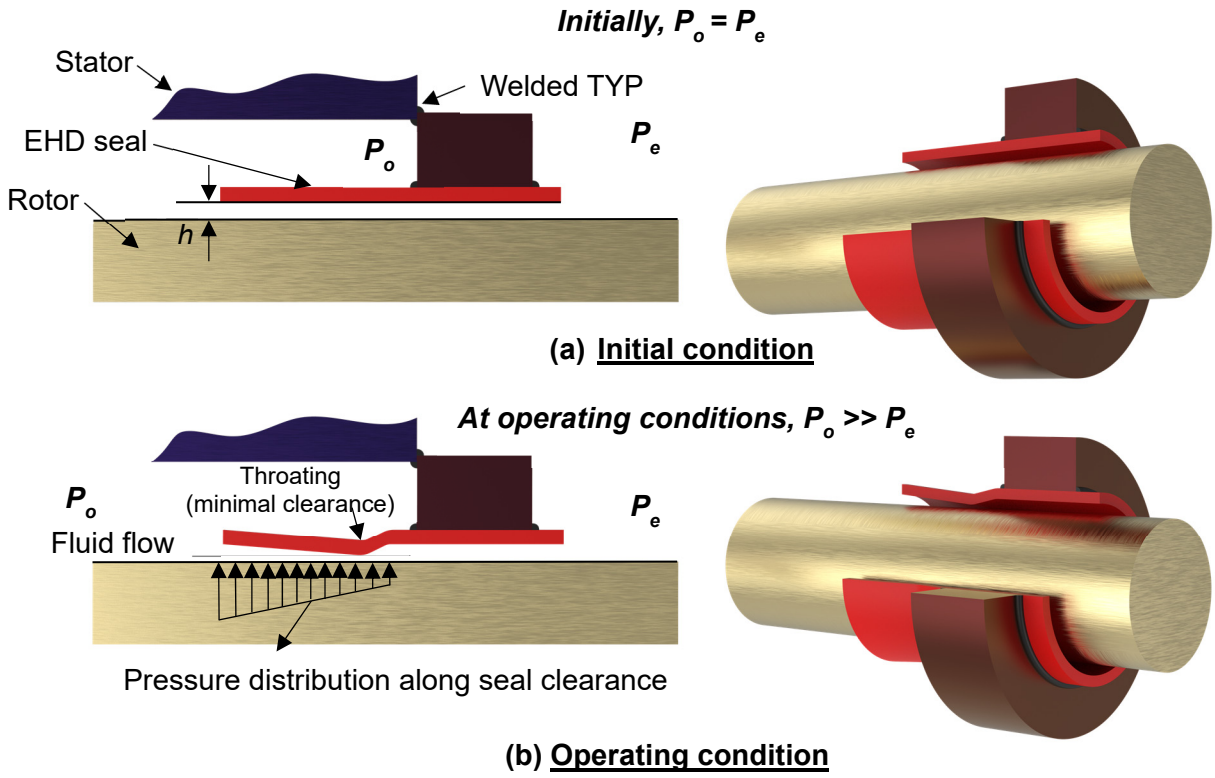

performance at critical speeds.

FIGURE 1: Working principle of the proposed sealing concept.

This paper presents an experimental approach to evaluate the elastohydrodynamic (EHD) mechanism of the seal design described in our research. The experimental setup consists of a stationary test apparatus that includes a nitrogen tank with a maximum pressure of 16.50 MPa, a cylindrical chamber housing the stationary shaft and the test seal, steel tubing equipped with compression-type fittings, a pressure sensor for measuring nitrogen pressure, and a mass flow meter. The static shaft utilized in the experiment was composed of 303 stainless steels. However, the test seal employed was constructed from PEEK plastic. The LabVIEW program measured the

pressure and temperature at the input and the outlet's mass flow rate. To facilitate the process of instrumentation, the integration of DAQ modules was carried out by incorporating them into a chassis that is compatible with the system. The studies were carried out with an initial clearance of 41 μm, and the inlet pressure was then raised to 15 MPa. The preliminary studies effectively elucidated the performance of the EHD seal in terms of throttling. The findings from this study suggest that the proposed EHD seal design can potentially be employed in supercritical carbon dioxide (sCO_2) turbomachinery.

MATERIALS AND METHODS

Proposed sealing concept

The proposed EHD seal modulates the demonstrated elastohydrodynamic lubrication sealing mechanism, eliminating wear, lowering leakage, and saving costs. The primary EHD seal is affixed to a back ring and positioned on a rotor with a preliminary clearance of "*h*", as shown in Figure 1. In this scenario, the operating pressure, "P_O", is the same as the environmental pressure, "P_e" ($P_O = P_e$). After the rotor ramps up, operating pressure increases. This results in $P_O >> P_e$ and the pressure distribution in the clearance decreases. The pressure at the top of the seal is equal to the operating pressure P_O.

As the seal is welded onto the back ring, the root of the seal is fixed. Eventually, the pressures at the top and bottom of the seal will settle for the least amount of feasible physical clearance between the rotor and the seal. The seal may bend downward and remain there, obstructing the flow. However, the pressure differential across the contact region will force the contact to reopen when interaction happens. Since the maximum working pressure will remain consistent, any oscillation will be restricted, limiting any instability until the seal opens again. Recall that during operation, P_O is always greater than P_e. Given the foregoing considerations, there will always be a minimal sustainable clearance between the rotor and the seal, acting as an efficient throttling mechanism to minimize the leakage.

EXPERIMENTAL SETUP

Test rig assembly

The test rig was methodically designed to effectively maintain gas pressure, ensuring that any observed reductions in pressure may be ascribed solely to the seal being subjected to testing. The design facilitates the efficient measurement of the leakage rate at the desired pressure. The desired outcome can be attained by establishing a regulated setting, including only one route for potential leakage, namely the clearance between the seal and the shaft. The existing experimental configuration was specifically designed to ensure the effective sealing of a stationary shaft. Figures 2 and 3 display schematic diagrams of the test rig.

The overall dimensions of the entire test rig, which is comparable to the size of a tabletop, do not exceed 12-in in length, 12-in in width, and 8-in in height. The shaft and seal components are contained within a tubular body with an inner diameter of 3.75", which is equipped with inlet and outlet flanges. The flanges were fastened with grade-8 partly threaded bolts and grade-8 hex nuts. The test rig's body is securely attached to the tabletop.

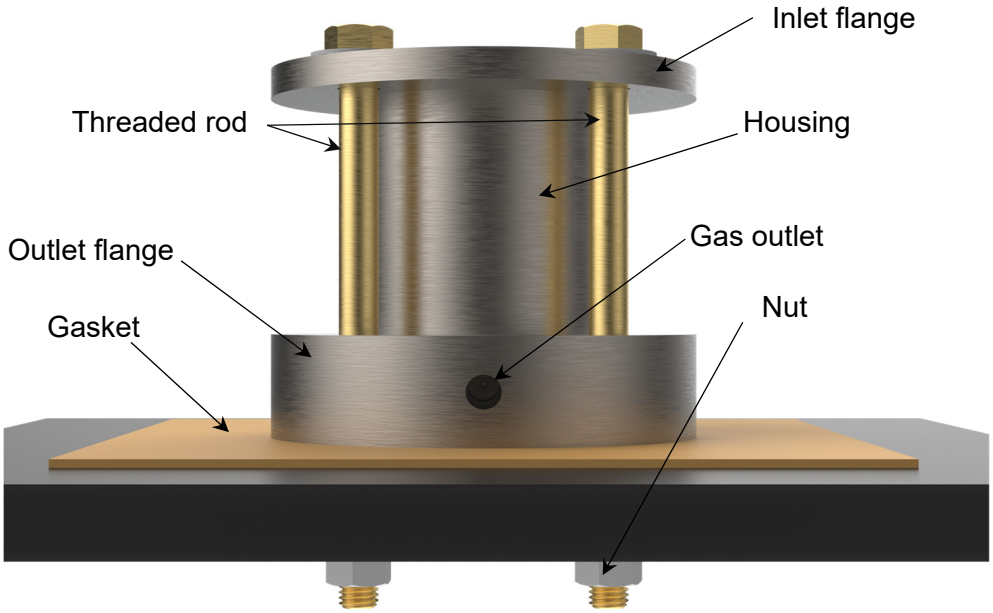

FIGURE 2: Assembled test rig for the experiment.

O-rings are employed to seal the inlet and outlet flanges while effectively mitigating parasitic leakage. The seal has been affixed to the outlet flange, creating a pathway for leakage via the shaft and subsequent release through the outlet flange. Figure 3 presents a cross-sectional depiction of the test rig, illustrating the essential components and the leakage pathway.

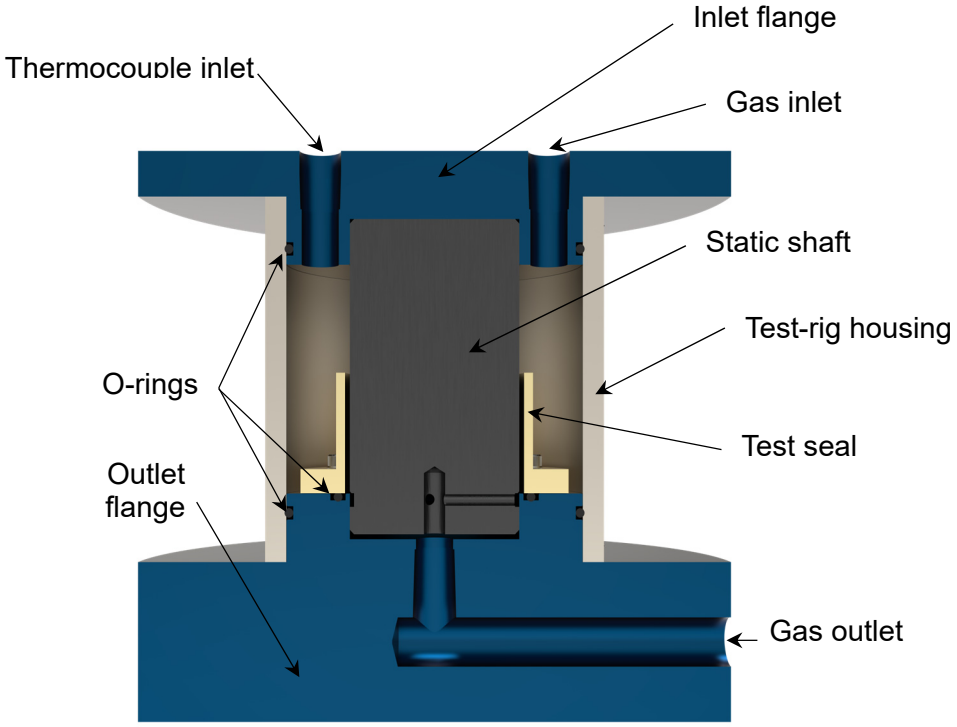

FIGURE 3: Cross-sectional view of the test rig.

Compression tube fittings are commonly employed in tubing applications. Flexible stainless-steel tubing, measuring 0.02-in thickness and ¼-in diameter, is employed to transfer gas from a gas cylinder of size 300 (which is designed to withstand pressures of 2,400 psi at a temperature of 72°F) to the chamber of the test rig.

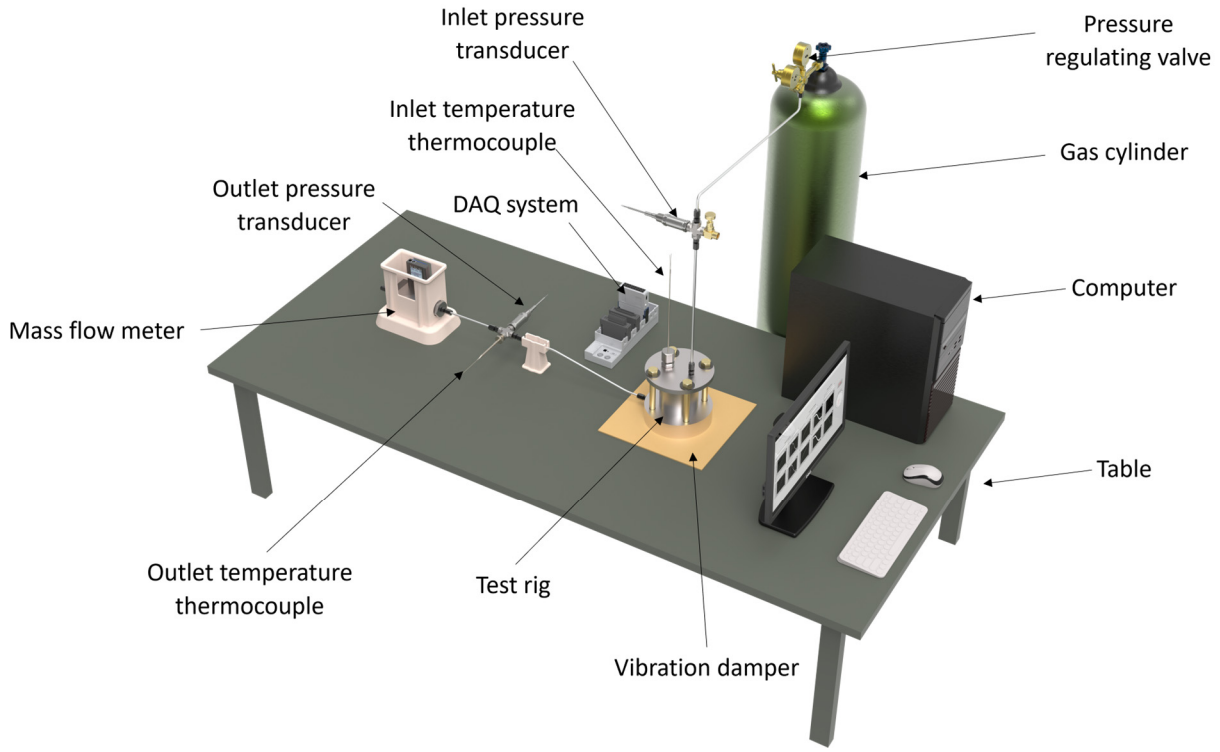

FIGURE 4: Schematic of the full experimental setup.

A gas regulator manages the gas flow at the inlet by being attached to the gas cylinder. All fittings used for gas supply are of the compression type. The inlet and output flanges have ¼-in NPT threaded holes that accommodate suitable adapters for compression fittings. A thin film pressure transducer that utilizes sputtering techniques is positioned near the inlet to measure the pressure provided to the gas chamber. An additional digital pressure gauge is installed at the outlet to serve as a safety mechanism and to monitor the pressure level at the outlet accurately. After exiting the test rig outlet, the gas being released will traverse through a mass flow rate meter. The mass flow rate meter will be utilized to quantify the rate of leakage occurring beneath the seal. Figure 4 comprehensively depicts the experimental arrangement, encompassing the test rig, tubing, gas cylinder and so on. Data monitoring system, and instrumental tools, together with their respective specifications are described in Tables 1-5/ Figure 5.

Data acquisition

A sputtered thin film pressure transducer was incorporated to measure the inlet pressure. The material can endure elevated temperature and pressure levels while also delivering an output signal measured in Volts. Most pressure transducers utilize strain gauge technology. The inner diaphragm contains minuscule strain gauges, which showcase a resistance alteration directly proportional to the magnitude of the applied pressure. For a pressure transducer to function, it necessitates an excitation voltage. A thermocouple composed of Inconel alloy with a length of 7.5-in and a K-type configuration was selected to measure the temperature change at the tip of

the seal. The sensor element of a thermocouple is composed of the alloy combination known as “Chromel/Alumel”, which offers a high-temperature tolerance ranging from -200°C to +1,260°C. A maximum sheath diameter of 0.125-in was selected for the thermocouple. When considering tip arrangement, utilizing a single ungrounded setup is recommended to measure gas or air temperature. The temperature measurement was concluded by employing fiberglass/silicone-impregnated lead wire insulation. The temperature thermocouple can provide data in the form of voltage output (V).

The mass flow rate meter is a crucial component to ensuring the effectiveness of experimental analysis. Recording and comparing leakage rates for different seals is eased by this approach, aiding in attaining the primary objective. FMA-1623AI mass flow rate meter was selected for estimating the leakage rate. It can measure mass flow within a specified range of 15-3,000 SLPM (standard liters per minute). But it doesn’t provide data as specific liters per minute. However, it can provide specific mass flow data in g/s for up to 30 g/s. It offers information in the form of current output (mA). FMA-1623AI can withstand a maximum of 145 psi inlet pressure.

A high-pressure thermocouple plug sensor of the model TC-K-NPT-U-72 was employed to monitor the temperature at the outlet. The sensor element is constructed using a combination of Chromel and Alumel, denoted as K type, to facilitate precise measurements within a specified operational temperature range from 0°C to +650°C (0°F to +1,200°F). The product is fabricated using resilient 304 Stainless steel, and the sensor is securely affixed using stainless steel mounting components. The thermocouple has a ¼-in NPT male mounting thread to facilitate convenient installation.

A PX409 series pressure transducer was employed for pressure monitoring at the exit. The transducers employ a comprehensive Wheatstone bridge configuration on a silicon wafer to ensure dependable stability, linearity, repeatability, and enduring durability. The input and output resistances are carefully controlled to fall within a standard range of 5,000 Ω ±20%, guaranteeing constant operational characteristics. The transducers offer precise pressure measurements with a maximum repeatability of ±0.08% of the full scale. Furthermore, these sensors possess adaptability in many environmental conditions, as evidenced by their ability to tolerate vibrations within a frequency spectrum ranging from 5 Hz to 2,000 Hz, with the capacity to return to a baseline of 5 Hz. The transducers are fabricated using robust 316L stainless steel material, which provides excellent resistance against corrosion. Additionally, these transducers reveal a remarkable overall accuracy of ±0.08%, hence significantly improving reliability for applications requiring high precision levels.

The compactDAQ chassis manages the timing, synchronization, and data transfer between the NI C Series I/O modules and an external host. It typically includes connectivity options such as usb, ethernet, or wifi. The chassis is equipped with multiple slot counts, enabling the simultaneous integration of an appropriate number of input or output interfaces for diverse applications. This project utilized a selection of C series input-output modules to acquire measurements, including an array of analog input/output and counter/timer functionalities. The compactDAQ chassis is equipped with various general-purpose counters/timers that can be accessed by means of a hardware-timed digital C series module inserted within the system. Such counters/timers are designed to cater to various applications. These applications encompass the utilization of quadrature encoders, pulse width modulation (PWM), event counting, pulse train production, as well as period or frequency monitoring. A notable characteristic of this technology is the provision of several timing engines, enabling users to execute numerous hardware-timed processes concurrently, each with distinct rates for analog input.

(a) Mass flow meter

TABLE 1: Specifications of the mass flow meter

Specification	Value
Flow range	15-3,000 SLPM
Accuracy	±0.8%
Output signal	4-20 mA
Fitting size	1 ¼-in
Power supply	110V AC
Maximum process temperature	+50˚C (+122˚F)

(b) Thermocouple and sealant assembly

TABLE 2: Specifications of the inlet thermocouple

Specification	Value
Sensor element	K Chromel/Alumel
Working temperature	-200 to +1,260˚C
Sheath material	Inconel 600
Mounting material	Stainless steel
Mounting thread	¼-in NPT male

(c) PX5500C0-2.5KA10E pressure transducer

TABLE 3: Specifications of the inlet pressure transducer

Specification	Value
Pressure range	0-2,500 Psi
Pressure type	Absolute
Accuracy value	±0.15%
Output signal	Voltage
Pressure port size	¼-in
Pressure port type	NPT male

(d) PX409-1-0KA10V pressure transducer

TABLE 4: Specifications of the outlet pressure transducer

Specification	Value
Pressure range	0-1,000 Psi
Pressure type	Absolute
Accuracy value	±0.08%
Output signal	Voltage
Pressure port size	¼-in
Pressure port type	NPT male

(e) TC-K-1-4NPT-U-72 thermocouple

TABLE 5: Specifications of the outlet thermocouple

Specification	Value
Sensor element	K Chromel/Alumel
Working temperature	0 to +650˚C
Sheath material	304 Stainless steel
Mounting material	Stainless steel
Mounting thread	¼-in NPT male

FIGURE 5: Instrumentation sensors and their specifications.

Table 6 indicates the instruments used for data acquisition, monitor and recording of the test. All the sensors for the EHD project are integrated into a single code, and LabVIEW was used to acquire and analyze data simultaneously. Below is the virtual interface of the LabVIEW code (Figures 6).

TABLE 6: List of DAQ modules and chassis

Part number	Description
NI-9205	C series voltage input module
NI-9212	C series temperature input module
TB-9212	Terminal block for NI-9212
NI-9253	C series current input module
cDAQ-9178	CompactDAQ chassis for input modules

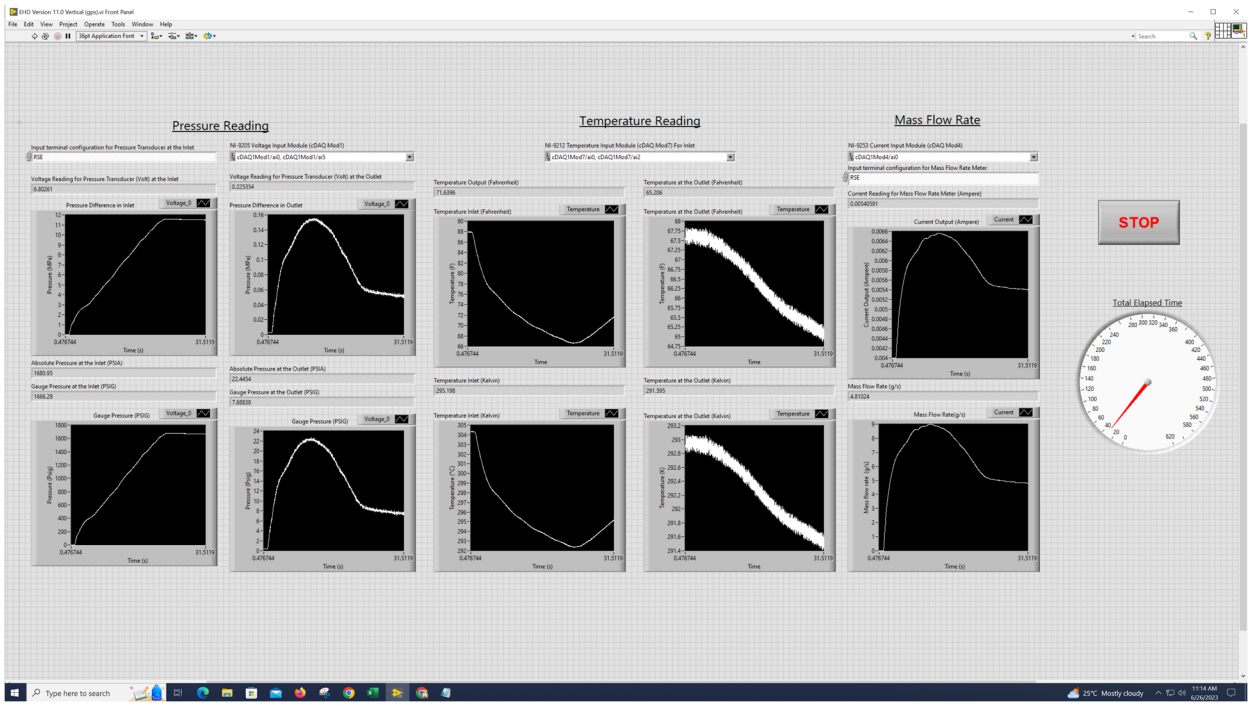

FIGURE 6: A representative virtual interface of the LabVIEW code. Note that the limited maximum tank pressure does now allow the leakage to reduce all the way down as in Figures 10 and 11. This might happen when the tank is not full.

Seal materials

A PEEK plastic seal was employed for the test (Figure 7). The seal measures 1-in length, 2.009-in inner diameter, and 0.096-in sleeve thickness. A flange with an exterior diameter of 3.00-in and a thickness of 0.25-in is used to attach the seal. Table 7 provides the material parameters of the seal material.

TABLE 7: Material properties of the seal material

Properties	Value
Flexural modulus	3.65 GPa
Hardness	Rockwell R126
Tensile strength	96.53 MPa
Temperature	-20° – 480° F
Coefficient of thermal expansion	0.2 – 0.4
Impact strength	0.6 – 0.95 ft-lbs/in
Thermal expansion	2.5 x 10 – 5 in/°F
Water absorption	0.10 – 0.45%

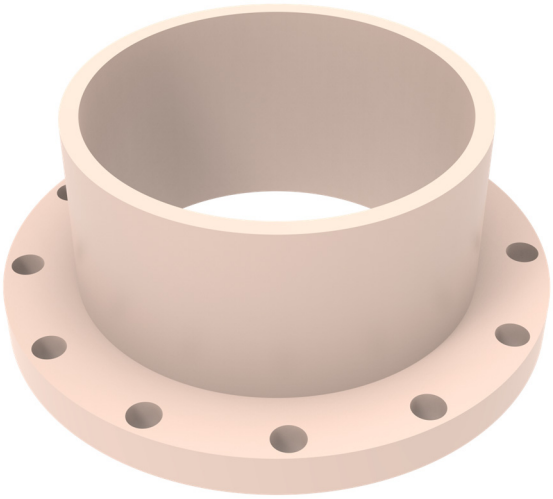

FIGURE 7: PEEK seal used in the experiment.

Statistical analysis

A statistical analysis was conducted to calculate the stochastic errors present in the experimental data to assess the reproducibility of the findings. Since six tests were undertaken in the experiment, it is worth noting that the sample size was relatively small. Consequently, the student's t-distribution was employed to estimate the confidence interval. Per the approach outlined by Wheeler and Ghanji [56], we performed calculations to determine the confidence interval for both the mean pressure difference (*P*) and the rate of leakage (*Q*). By employing this methodology, we evaluated the degree of uncertainty linked to our findings and ascertained the statistical significance of the observed disparities. The inclusion of statistical analysis is of utmost importance in guaranteeing the integrity and dependability of experimental outcomes, especially in cases involving limited sample sizes. This analytical process addresses the influence of chance fluctuations and measurement inaccuracies that may compromise the precision of the results. The equation to calculate the stochastic error is as follows:

$$\bar{x} \pm t_{\alpha/2} \frac{S}{\sqrt{n}} \qquad (1)$$

Where, $\bar{x}$ refers as the sample mean, $t_{\alpha/2}$ is the critical value, α=0.05 is the level of significance, S as the sample standard deviation and n=6 is the number of sample. This approach allowed us to assess the level of uncertainty associated with the results and to determine whether the observed differences were statistically significant.

Experimental procedure

Prior to conducting the tests, a standardized protocol is implemented to mitigate potential human errors and lessen the likelihood of inadvertent incidents. It also helped to ensure that all testing is conducted in a standardized and controlled environment. Since several experimental tests are subject to the influence of various uncontrollable parameters, adhering to a systematic and predetermined sequential approach mitigates and accounts for these parameters.

In our experiments, the seal dimensions were initially assessed using a coordinate measurement machine (Figure 8). The seal's inner diameter, outer diameter, flange thickness,

seal thickness, cylindricity, seal height, flange diameter, and screw hole positions were measured and recorded. Subsequently, the test seal was affixed onto the outlet flange, with the static shaft passing through it, and the seal positions were secured employing six socket head screws. A dial torque wrench was utilized to achieve a consistent torque of 5lb-in on each of the six screws.

FIGURE 8: Seal dimensions measurement using CMM machine.

Afterward, the remaining components of the test rig were assembled, followed by the integration of the sensors. It was verified that the emergency ball valve was in a closed position. The power supply was connected and activated by turning on the excitation voltage switches. The USB cord linked to the data monitoring computer was also inspected. The LabVIEW code was executed to assess the functionality of all sensors.

The next step involved the replacement of the gas tank. A fresh nitrogen tank was employed daily to conduct successive rounds of experiments. Upon establishing a connection between the gas regulator and the nitrogen tank, the valve of the tank was opened afterward to ascertain whether the dial of the regulator accurately displayed the pressure within the tank. Later, the pressure of the test rig was elevated to 1 MPa to perform a leakage test.

After confirming the system was leak-proof, the actual tests were conducted. The gas regulator was manually regulated to raise the inlet pressure of the test rig. Typically, the operating pressure was elevated to 15 MPa. Considerable attention was given to the output pressure to prevent potential harm to the mass flow meter. To minimize the effect of initial temperature on the seal, 1.5 hr intervals were allowed between two recordings so that the temperature could return to room temperature. The sequential experimental methodology is indicated in Figure 9.

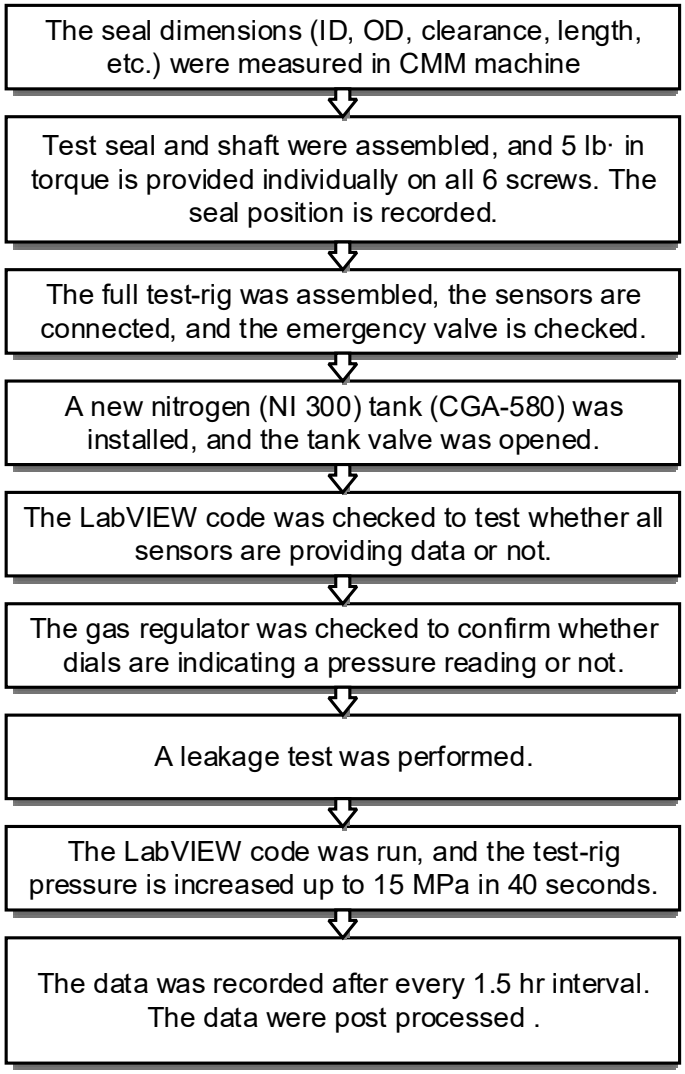

FIGURE 9: Flowchart for the experimental process.

RESULTS AND DISCUSSIONS

The measured relationship between the mass flow rate and operating pressure is shown in Figure 10. The correlation between the volume flow rate and operating pressure is shown in Figure 11. In this experiment, we measured the leakage rate at different pressure differences and calculated the average of six test values. We then determined the standard deviation of the data. The x-axis represents the pressure difference, and the y-axis represents the leakage rate (mass flow rate/ volume flow rate). As seen in Figures 10 and 11, the leakage rate increases linearly as the pressure increases until about 6 MPa because, at this stage, the seal is subjected to slight to no elastic deformation; therefore, there is barely any change in the flow area in the clearance. In other words, the seal behaves like a typical clearance-type seal.

In case of the average values (Figure 10), The maximum leakage rate recorded was 4.49 g/s at 6 MPa. The leakage rate then began dropping to 0.43 g/s as the pressure rose to 15 MPa, generating a bell-shaped curve. At a 95% confidence level, the estimated confidence intervals for the mean were ±0.12 g/s and ±0.09 g/s, respectively, for pressures of 6 MPa and 15 MPa

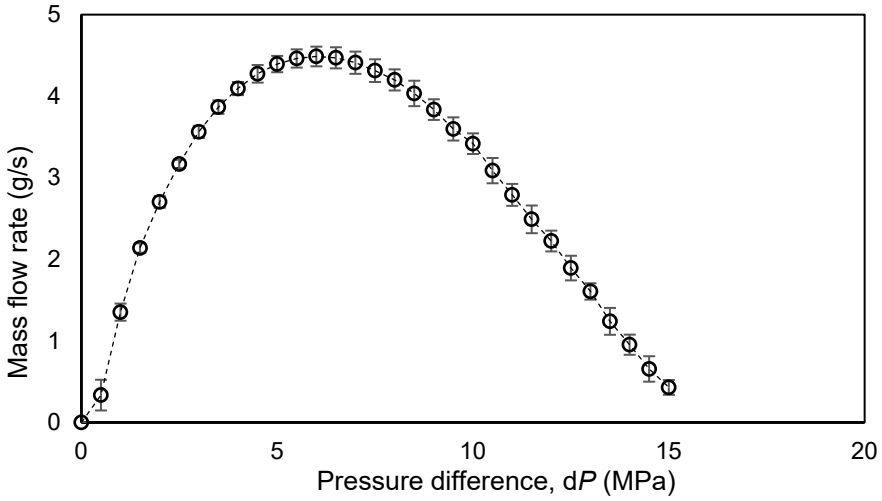

FIGURE 10: Mass flow rate and operating pressure averaged data.

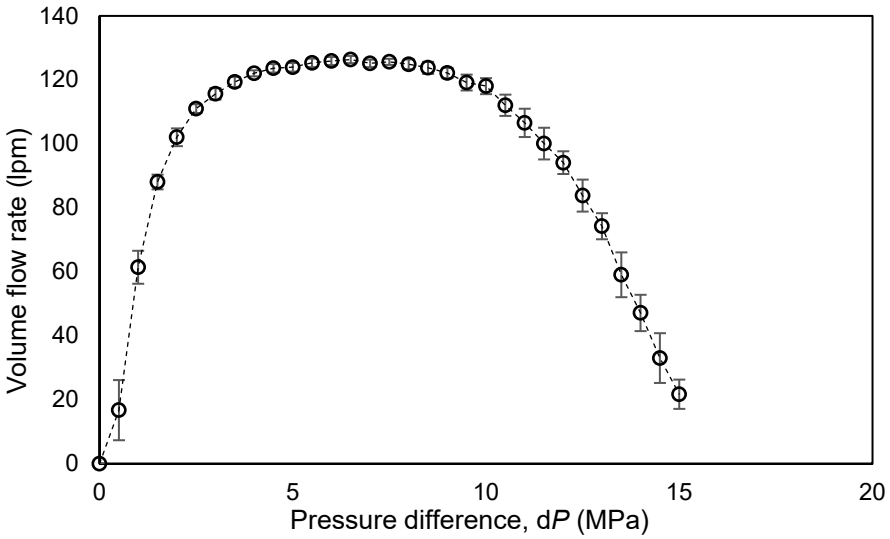

FIGURE 11: Volume flow rate and operating pressure averaged data.

As shown in Figure 11, the maximum volume flow rate recorded was 125.90 lpm at 6 MPa. The leakage rate then began dropping to 21.72 lpm as the pressure rose to 15 MPa, generating a bell-shaped curve. At a 95% confidence level, the estimated confidence intervals for the mean were ±1.27 lpm and ±4.57 lpm, respectively, for pressures of 6 MPa and 15 MPa. The throttling effect of the EHD seal was effectively established in early trials. The throat in the clearance acts as a flow restrictor, creating a significant drop in the pressure across the throat. The pressure recovery after the throat decreases with increasing operation pressures. Because the throttling effect, i.e., the reduction in the clearance height, becomes more robust with increasing operating pressures. The experimental observation here is also supported by the previous computational works conducted by other researchers [10], [11], [57]–[61]

Nevertheless, a minor disparity exists in the recorded flow rate and pressure data, giving rise to various potential factors that may account for this inconsistency. The primary factor contributing to the uncertainty in the outcomes is the presence of slight deviations in test results. This

phenomenon may arise from the alignment and integration of the mechanical components, as commonly observed in a conventional mechanical system, due to the significant overlap between the two subsequent tests. It is essential to acknowledge that the data reported in this study pertains to preliminary test outcomes. External influences, such as ambient temperature variations, may influence the observed disparities in flow rate measurements. Additional experimentation will be undertaken with alternative materials possessing greater rigidity and varying dimensions. Furthermore, an outlet will be equipped with a temperature sensor and a pressure sensor to facilitate the collection of volume flow rate data. However, the observed throttling behavior of the EHD seal in experimental studies shows promise and justifies the need for additional exploration. A full video demonstration of the experimental process was uploaded in YouTube which is accessible through this link.

CONCLUSIONS

A novel elastohydrodynamic (EHD) seal for sCO_2 application was proposed that demonstrated the ability to maintain a low leakage rate and minimal wear. Although PEEK was used for conducting the test, the goal is to use Inconel-718 as the seal material so that it can withstand high pressure and temperature working conditions. An experimental study for a 2-in test seal was presented. The primary findings of this study can be succinctly described as follows:

- The EHD seal throttled the leakage rate successfully.
- The investigation yielded a maximum average mass flow rate of 4.49 g/s at about 6 MPa.
- The average mass flow rate exhibited a downward trend as the operating pressures increased. The leakage rate was obtained to be 0.43 g/s at the maximum operating pressure of 15 MPa.
- The highest average volume rate observed was 125.90 lpm at around 6 MPa.
- The average volume flow rate continued to decrease with increasing operating pressures. The volume flow rate was 21.72 lpm at the maximum operating pressure of 15 MPa.
- The distinctive behavior exhibited by the EHD seal has potential benefits for sCO_2 turbomachinery applications, particularly in situations that demand reduced leakage rates under elevated pressure and temperature conditions.

The proposed EHD seal possesses sealing mechanisms that make it highly suitable for usage in the power industry, particularly in turbomachinery. It can potentially outperform existing seals such as brush, finger, compliant foil, and labyrinth seals in its capacity to control fluid loss and sustain a minimal film thickness. It outperforms in a sense that no other seal has shown the bell curve formation in their leakage vs pressure data. The leakage for the clearance type seals increases with increasing pressure; however, the leakage for the EHD seal reduces with increasing pressure after a certain pressure. With this unique feature, the EHD seal can potentially offer:

- **Low friction:** The EHD seal exhibits low friction characteristics due to its non-contact nature. This attribute contributes to the reduction of energy consumption and the enhancement of turbomachinery efficiency during operation.
- **Extended operating life:** It offers an extended operational life due to the absence of direct contact between the seal and shaft, limiting wear and tear.
- **Minimal leakage:** The EHD seal's dynamic throttling capacity reduces leakage and enhances overall efficiency.
- **Reduced maintenance costs:** One advantage of the EHD seal is its ability to lower maintenance costs. This is due to its uncomplicated design, which leads to lower starting

expenses and a longer operational lifespan. Consequently, the EHD seal may effectively minimize maintenance charges over an extended period.

- **Versatile applications:** The EHD seal illustrates the versatility and deems application in various turbomachinery systems, including compressors, gas turbines, steam turbines, and aviation engines. Moreover, these devices indicate compatibility with high pressure and challenging conditions.

Hence, incorporating EHD seals in turbomachinery within the power sector has a range of possible benefits, such as improved operational efficiency, reduced maintenance costs, and extended equipment longevity. The outstanding attributes possessed by these entities render them suitable for various applications and operational circumstances, as exemplified by their utilization in sCO_2 turbomachinery.

FUTURE STUDIES

As for future work, the following will be attempted to understand the EHD seal behavior better:

- The temperature effects were neglected in these initial experiments. In the next phase of experiments, the N_2 gas will be heated via resistant heaters prior to entering the seal clearance.

- The deformation on the seal will be measured via a series of strain gages. The effects of seal material and geometry will be analyzed by carrying out the tests using the seal's different types, i.e., materials and dimensions.

ACKNOWLEDGMENTS

The U.S. Department of Energy (DOE) has supported this study through Small Business Technology Transfer Research (STTR) Phase I and II awards under Grant No. DE-SC0020851. The Principal Investigator for the grant is Dr. Sevki Cesmeci and Dr. Hanping Xu serves as the Business Official. The financial assistance provided by the Department of Energy (DOE) is gratefully appreciated.

Disclaimer: This manuscript solely represents the perspectives of the author(s) and does not necessarily represent the viewpoints or opinions of the Department of Energy (DOE). The proposed seal concept's intellectual property is safeguarded by Patent No. 63/200,712, titled "Clearance seal with an externally pressurized sleeve."

REFERENCES

[1] M. Kulhánek and V. Dostál, “Supercritical Carbon Dioxide Cycles Thermodynamic Analysis and Comparison,” *Proc. SCCO2 Power Cycle Symp.*, pp. 1–12, 2011.

[2] M. S. Kim, Y. Ahn, B. Kim, and J. I. Lee, “Study on the supercritical CO2 power cycles for landfill gas firing gas turbine bottoming cycle,” *Energy*, vol. 111, pp. 893–909, 2016, doi: 10.1016/j.energy.2016.06.014.

[3] A. Thatte, A. Loghin, E. Martin, V. Dheeradhada, Y. Shin, and B. Ananthasayanam, “Multi-Scale Coupled Physics Models and Experiments for Performance and Life Prediction of Supercritical CO2 Turbomachinery Components,” *5th Int. Symp. - sCO2 Power Cycles*, vol. 1, pp. 1–24, 2016.

[4] M. Wolf and M. Anderson, “Experiment and Numerical Study of Supercritical Carbon

Dioxide Flow," no. Sneck 1974, 2014.
[5] J. Cho *et al.*, "Development of the supercritical carbon dioxide power cycle experimental loop in kier," *Proc. ASME Turbo Expo*, vol. 9, 2016, doi: 10.1115/GT2016-57460.
[6] J. E. Cha, S. W. Bae, J. Lee, S. K. Cho, J. I. Lee, and J. H. Park, "Operation Results of a Closed Supercritical CO2 Simple Brayton Cycle," *5th Int. Supercrit. CO2 Power Cycles Symp.*, pp. 1–10, 2016, [Online]. Available: https://sci-hub.st/http://sco2symposium.com/papers2016/Testing/085paper.pdf
[7] D. Steinmann *et al.*, "The 7th International Supercritical CO2 Power Cycles Symposium Dry Gas Seals Design for Centrifugal Compressors in Supercritical CO2 Application," pp. 1–24, 2022.
[8] E. Anselmi, V. Pachidis, M. Johnston, I. Bunce, and P. Zachos, "An Overview of the Rolls-Royce sCO2 -Test Rig Project at Cranfield," *6th Int. Symp. - Supercrit. CO2 Power Cycles*, 2018.
[9] M. T. White, G. Bianchi, L. Chai, S. A. Tassou, and A. I. Sayma, "Review of supercritical CO2 technologies and systems for power generation," *Appl. Therm. Eng.*, vol. 185, p. 116447, 2021.
[10] K. R. Lyathakula, S. Cesmeci, M. F. Hassan, H. Xu, and J. Tang, "A Proof-of-Concept Study of a Novel Elasto-Hydrodynamic Seal for CO2," in *ASME Power Conference*, American Society of Mechanical Engineers, 2022, p. V001T12A003.
[11] S. Cesmeci, K. R. Lyathakula, M. F. Hassan, S. Liu, H. Xu, and J. Tang, "Analysis of an Elasto-Hydrodynamic Seal by Using the Reynolds Equation," *Appl. Sci.*, vol. 12, no. 19, p. 9501, 2022.
[12] C. M. G. Tech, S. B. Drive, N. York, and J. C. Dudley, "FILM RIDING LEAF SEALS FOR IMPROVED SHAFT SEALING Clayton," *ASME Turbo Expo*, no. 978-0-7918-4399–4, pp. 1293–1300, 2010, doi: https://doi.org/10.1115/GT2010-23629.
[13] H. Jin, "A REDUCED-ORDER MODEL FOR ANNULAR LABYRINTH SEALS BASED ON PROPER ORTHOGONAL DECOMPOSITION," *ASME 2016 Int. Mech. Eng. Congr. Expo.*, vol. V007T09A03, no. 978-0-7918-5061–9, pp. 1–8, 2016, doi: https://doi.org/10.1115/IMECE2016-67086.
[14] A. Untaroiu *et al.*, "Fluid-induced forces in pump liquid seals with large aspect ratio," *ASME-JSME-KSME 2011 Jt. Fluids Eng. Conf. AJK 2011*, vol. 1, no. PARTS A, B, C, D, pp. 455–463, 2011, doi: 10.1115/AJK2011-06085.
[15] S. Liu, Q. J. Wang, Y. W. Chung, and S. Berkebile, "Lubrication–Contact Interface Conditions and Novel Mixed/Boundary Lubrication Modeling Methodology," *Tribol. Lett.*, vol. 69, no. 4, pp. 1–23, 2021, doi: 10.1007/s11249-021-01515-w.
[16] H. Nami, S. M. S. Mahmoudi, and A. Nemati, "Exergy, economic and environmental impact assessment and optimization of a novel cogeneration system including a gas turbine, a supercritical CO2 and an organic Rankine cycle (GT-HRSG/SCO2)," *Appl. Therm. Eng.*, vol. 110, pp. 1315–1330, 2017, doi: 10.1016/j.applthermaleng.2016.08.197.
[17] H. Jin, A. Untaroiu, and G. Fu, "Effect of surface patterning on the dynamic response of annular hole-pattern seals," *Proc. ASME Turbo Expo*, vol. 7A-2017, pp. 1–10, 2017, doi: 10.1115/GT201764875.
[18] Y. Liu, B. Yue, X. Kong, H. Chen, and H. Lu, "Effects of Front Plate Geometry on Brush Seal in Highly Swirling Environments of Gas Turbine," *Energies*, 2021.
[19] F. E. Aslan-zada, V. A. Mammadov, and F. Dohnal, "Brush seals and labyrinth seals in gas turbine applications," *Proceedings of the Institution of Mechanical Engineers, Part A: Journal of Power and Energy*, vol. 227, no. 2. pp. 216–230, Mar. 2013. doi: 10.1177/0957650912464922.
[20] Y. Liu, B. Yue, X. Kong, H. Chen, and H. Lu, "Effects of Front Plate Geometry on Brush Seal in Highly Swirling Environments of Gas Turbine," *Energies*, vol. 14, no. 22, p. 7768, 2021.

[21] N. Sarawate and D. Trivedi, “Rotating brush Seal design and performance testing,” in *Turbo Expo: Power for Land, Sea, and Air*, American Society of Mechanical Engineers, 2021, p. V05BT14A001.
[22] E. T. Duran, “Brush seal contact force theory and correlation with tests,” *Alexandria Eng. J.*, vol. 61, no. 4, pp. 2925–2938, 2022.
[23] R. E. Chupp, F. Ghasripoor, N. A. Turnquist, M. Demiroglu, and M. F. Aksit, “Advanced seals for industrial turbine applications: Dynamic seal development,” *J. Propuls. Power*, vol. 18, no. 6, pp. 1260–1266, 2002, doi: 10.2514/2.6061.
[24] T. Yuan, Z. Li, J. Li, and Q. Yuan, “Static and Rotordynamic Characteristics for Supercritical Carbon Dioxide Spiral Groove Dry Gas Seal With the Tilted Seal Ring,” *J. Eng. Gas Turbines Power*, vol. 145, no. 1, p. 11011, 2023.
[25] H. Heshmat, J. F. Walton II, and J. L. Córdova, “Technology Readiness of 5th and 6th Generation Compliant Foil Bearing for 10 MWE S-CO2 Turbomachinery Systems,” in *The 6th International Supercritical CO2 Power Cycles Symposium*, 2018, pp. 1–29.
[26] R. A. Bidkar *et al.*, “Low-Leakage Shaft-End Seals for Utility-Scale Supercritical CO2 Turboexpanders,” *J. Eng. Gas Turbines Power*, vol. 139, no. 2, pp. 1–8, 2017, doi: 10.1115/1.4034258.
[27] H. Xu and T. Lei, “A ringless high pressure moving seal up to 1200 mpa,” *Tribol. Trans.*, vol. 37, no. 4, pp. 767–770, 1994, doi: 10.1080/10402009408983358.
[28] L. S. Andres, T. Wu, J. Barajas-Rivera, J. Zhang, and R. Kawashita, “Leakage and cavity pressures in an interlocking labyrinth gas seal: Measurements versus predictions,” *J. Eng. Gas Turbines Power*, vol. 141, no. 10, pp. 1–9, 2019, doi: 10.1115/1.4044284.
[29] A. Bowsher, P. Crudgington, C. M. Grondahl, J. C. Dudley, T. Kirk, and A. Pawlak, “Pressure Activated Leaf Seal Technology Readiness Testing,” *J. Eng. Gas Turbines Power*, vol. 137, no. 6, pp. 1–13, 2015, doi: 10.1115/1.4028678.
[30] N. R. Morgan, A. Untaroiu, P. J. Migliorini, and H. G. Wood, “Design of experiments to investigate geometric effects on fluid leakage rate in a balance drum seal,” *J. Eng. Gas Turbines Power*, vol. 137, no. 3, pp. 1–8, 2015, doi: 10.1115/1.4028382.
[31] P. J. Migliorini, A. Untaroiu, and H. G. Wood, “A numerical study on the influence of hole depth on the static and dynamic performance of hole-pattern seals,” *J. Tribol.*, vol. 137, no. 1, pp. 1–7, 2015, doi: 10.1115/1.4028604.
[32] P. J. Migliorini, A. Untaroiu, W. C. Witt, N. R. Morgan, and H. G. Wood, “Hybrid analysis of gas annular seals with energy equation,” *J. Tribol.*, vol. 136, no. 3, pp. 1–9, 2014, doi: 10.1115/1.4026590.
[33] D. Trivedi, R. A. Bidkar, C. E. Wolfe, and J. Mortzheim, “Supercritical CO2 Tests for Hydrostatic Film Stiffness in Film-Riding Seals,” in *Turbo Expo: Power for Land, Sea, and Air*, American Society of Mechanical Engineers, 2019, p. V009T38A018.
[34] S. Cesmeci *et al.*, “An Innovative Elasto-Hydrodynamic Seal Concept for Supercritical CO2 Power Cycles,” *ASME 2021 Power Conf. 2021*, no. V001T04A002, pp. 1–10, 2021, doi: https://doi.org/10.1115/POWER2021-64536.
[35] J. F. Justak and C. Doux, “SELF-ACTING CLEARANCE CONTROL FOR TURBINE BLADE OUTER AIR SEALS,” *ASME Turbo Expo*, vol. 3, no. ISBN: 978-0-7918-4884-5, p. 9, 2009, doi: https://doi.org/10.1115/GT2009-59683.
[36] J. G. Ferguson, “Brushes As High Performance Gas Turbine Seals.,” *Am. Soc. Mech. Eng.*, 1988, doi: 10.1115/88-gt-182.
[37] H. Zhao, H. Su, and G. Chen, “Analysis of total leakage of finger seal with side leakage flow,” *Tribol. Int.*, vol. 150, no. March, p. 106371, 2020, doi: 10.1016/j.triboint.2020.106371.
[38] A. Laxander, A. Fesl, and B. Hellmig, “Development And Testing Of Dry Gas Seals For Turbomachinery In Multiphase CO2 Applications,” *3rd Eur. Supercrit. CO2 Conf.*, pp. 1–12, 2019, doi: 10.17185/duepublico/48878.
[39] D. Dowson, “A generalized Reynolds equation for fluid-film lubrication,” *Int. J. Mech. Sci.*,

vol. 4, no. 2, pp. 159–170, 1962, doi: 10.1016/S0020-7403(62)80038-1.
[40] J. Nielson *et al.*, “Component Testing of a High Temperature Dry Gas Seal,” pp. 1–14, 2022.
[41] H. G. W. Patrick J. Migliorini∗, Alexandrina Untaroiu, William C. Witt, Neal R. Morgan, “HYBRID ANALYSIS OF GAS ANNULAR SEALS WITH ENERGY EQUATION,” *J. Tribol.*, vol. 136(3), no. 031704, pp. 1–10, 2017, doi: https://doi.org/10.1115/1.4026590.
[42] A. Untaroiu, H. G. Wood, and P. E. Allaire, “NUMERICAL MODELING OF FLUID-INDUCED ROTORDYNAMIC FORCES IN SEALS WITH LARGE ASPECT RATIO Alexandrina,” *J. Eng. Gas Turbines Power*, vol. 135(1), no. 012501, pp. 1–9, 2016, doi: https://doi.org/10.1115/1.4007341.
[43] S. L. Seals, C. P. Goyne, C. D. Untaroiu, H. G. Wood, and P. E. Allaire, “IMECE2008-6 7847,” pp. 1–7, 2016.
[44] B. K. M. Zickuhr, “Demonstration testing and facility requirements for sCO2 Brayton Commercialization,” no. June, 2016.
[45] A. Untaroiu, N. Morgan, V. Hayrapetian, and B. Schiavello, “Dynamic response analysis of balance drum labyrinth seal groove geometries optimized for minimum leakage,” *J. Vib. Acoust.*, vol. 139, no. 2, 2017, doi: 10.1115/1.4035380.
[46] A. Rimpel *et al.*, “Test rig design for large supercritical CO2 turbine seals,” *6th Int. Symp. - Supercrit. CO2 Power Cycles*, pp. 1–14, 2018.
[47] Z. Wang, B. Zhang, Y. Chen, S. Yang, H. Liu, and H. Ji, “Investigation of Leakage and Heat Transfer Properties of the Labyrinth Seal on Various Rotation Speed and Geometric Parameters,” *Coatings*, vol. 12, no. 5, p. 586, 2022.
[48] A. Untaroiu, H. Jin, G. Fu, V. Hayrapetiau, and K. Elebiary, “The Effects of Fluid Preswirl and Swirl Brakes Design on the Performance of Labyrinth Seals,” *J. Eng. Gas Turbines Power*, vol. 140, no. 8, pp. 1–9, 2018, doi: 10.1115/1.4038914.
[49] T. Yuan, R. Yang, Z. Li, J. Li, Q. Yuan, and L. Song, “Thermal characteristics and cooling effect for SCO2 dry gas seal with multiple dynamic groove types,” *Appl. Therm. Eng.*, vol. 236, no. PD, p. 121896, 2024, doi: 10.1016/j.applthermaleng.2023.121896.
[50] X. Wang, M. Liu, S. Kao-Walter, and X. Hu, “Numerical evaluation of rotordynamic coefficients for compliant foil gas seal,” *Appl. Sci.*, vol. 10, no. 11, p. 3828, 2020.
[51] G. K. Nikas and R. S. Sayles, “Nonlinear elasticity of rectangular elastomeric seals and its effect on elastohydrodynamic numerical analysis,” *Tribol. Int.*, vol. 37, no. 8, pp. 651–660, 2004, doi: 10.1016/j.triboint.2004.02.002.
[52] G. K. Nikas, “Elastohydrodynamics and mechanics of rectangular elastomeric seals for reciprocating piston rods,” *J. Trib.*, vol. 125, no. 1, pp. 60–69, 2003.
[53] G. K. Nikas, “Elastohydrodynamics and mechanics of rectangular elastomeric seals for reciprocating piston rods,” *J. Tribol.*, vol. 125, no. 1, pp. 60–69, 2003, doi: 10.1115/1.1506316.
[54] S. Stupkiewicz and A. Marciniszyn, “Elastohydrodynamic lubrication and finite configuration changes in reciprocating elastomeric seals,” *Tribol. Int.*, vol. 42, no. 5, pp. 615–627, 2009, doi: 10.1016/j.triboint.2008.08.008.
[55] P. L. Wong, H. Xu, and Z. Zhang, “Performance evaluation of high pressure sleeve seal,” *Wear*, vol. 210, no. 1–2, pp. 104–111, 1997, doi: 10.1016/S0043-1648(97)00050-1.
[56] A. R. Wheeler, A. J., and Ganji, “No Title,” *2010, Introd. to Eng. Exp. 3rd ed., Pearson High. Educ. Up. Saddle River, NJ, Chap. 6-7*.
[57] L. KR, C. S, D. M, & Xu H, and T. J., “Physics-Informed Deep Learning-Based Modeling of a Novel Elastohydrodynamic Seal for Supercritical CO2 Turbomachinery,” in *ASME 2022 Power Conference*, 2022.
[58] S. Cesmeci *et al.*, “An Innovative Elasto-Hydrodynamic Seal Concept for Supercritical CO2 Power Cycles,” pp. 1–10, 2021.
[59] L. KR, C. S, H. MF, X. H, and T. J, “A Proof-of-Concept Study of a Novel Elasto-

Hydrodynamic Seal for Supercritical CO2 Turbomachinery Applications," in *ASME 2022 Power Conference*, 2022.
[60] S. Cesmeci, K. R. Lyathakula, M. F. Hassan, S. Liu, H. Xu, and J. Tang, "Analysis of an Elasto-Hydrodynamic Seal by Using the Reynolds Equation," *Appl. Sci.*, vol. 12, no. 19, p. 9501, 2022, doi: 10.3390/app12199501.
[61] S. Cesmeci *et al.*, "An Innovative Elasto-Hydrodynamic Seal Concept for Supercritical CO2 Power Cycles," in *ASME 2021 Power Conference*, 2021, p. V001T04A002. doi: https://doi.org/10.1115/POWER2021-64536.